

Article

Improvement of Filler Wire Dilution Using External Oscillating Magnetic Field at Full Penetration Hybrid Laser-Arc Welding of Thick Materials

Ömer Üstündağ^{1,2,*} , Vjaceslav Avilov³, Andrey Gumenyuk^{1,2}  and Michael Rethmeier^{1,2,4} 

¹ Bundesanstalt für Materialforschung und -prüfung, Unter den Eichen 87, 12205 Berlin, Germany; andrey.gumenyuk@bam.de (A.G.); michael.rethmeier@bam.de (M.R.)

² Fraunhofer Institute for Production Systems and Design Technology, Pascalstraße 8-9, 10587 Berlin, Germany

³ Institute of Materials and Joining Technology, Otto von Guericke Universität Magdeburg, Universitätsplatz 2, 39016 Magdeburg, Germany; avilov1948@gmail.com

⁴ Institute of Machine Tools and Factory Management, Technische Universität Berlin, Pascalstraße 8-9, 10587 Berlin, Germany

* Correspondence: oemer.uestuendag@ipk.fraunhofer.de; Tel.: +49-30-3900-6440

Received: 29 April 2019; Accepted: 21 May 2019; Published: 23 May 2019



Abstract: Hybrid laser-arc welding offers many advantages, such as deep penetration, good gap bridge-ability, and low distortion due to reduced heat input. The filler wire which is supplied to the process is used to influence the microstructure and mechanical properties of the weld seam. A typical problem in deep penetration high-power laser beam welding with filler wire and hybrid laser-arc welding is an insufficient mixing of filler material in the weld pool, leading to a non-uniform element distribution in the seam. In this study, oscillating magnetic fields were used to form a non-conservative component of the Lorentz force in the weld pool to improve the element distribution over the entire thickness of the material. Full penetration hybrid laser-arc welds were performed on 20-mm-thick S355J2 steel plates with a nickel-based wire for different arrangements of the oscillating magnetic field. The Energy-dispersive X-ray spectroscopy (EDS) data for the distribution of two tracing elements (Ni and Cr) were used to analyze the homogeneity of dilution of the filler wire. With a 30° turn of the magnetic field to the welding direction, a radical improvement in the filler material distribution was demonstrated. This would lead to an improvement of the mechanical properties with the use of a suitable filler wire.

Keywords: hybrid laser-arc welding; oscillating magnetic field; electromagnetic stirring; filler wire dilution; thick materials; full-penetration

1. Introduction

The hybrid laser-arc welding (HLAW) process is appropriate for the welding of thick metals due to the high energy of the laser beam which causes a deep penetration, high gap bridge-ability, and low distortion due to reduced heat input compared to arc-based welding processes. The coupling of the laser beam and arc within just one heating zone was developed at the end of the 1970s as arc augmented laser welding [1]. Since the 2000s, the HLAW of thick-walled steels is used in industrial applications such as shipbuilding [2], crane construction, and pipeline manufacturing [3].

Although high-power laser systems in a power range of 10 to 100 kW are available on the market, the application of HLAW for thick sections is still far from being implemented on an industrial scale, and remains restricted to a small number of cases, mostly where the thickness of the parts does not exceed 15 mm due to certain technological limitations. One of the limiting factors is the formation of gravitational drop-outs when welding thick materials, especially in a flat position (1G).

Therefore, arc-based welding processes are commonly used for the welding of thick-walled structures. These welding processes are less productive when compared to laser beam welding (LBW) or HLAW due to a lower penetration depth. In order to weld thick plates, multi-layer technology is used, which leads to high heat inputs and distortion of the plates. A rework such as flame straightening is time- and cost-consuming.

Several studies were conducted to investigate and increase the weldable material thickness for HLAW. The latest developments and trends in high-power laser beam welding are described in detail in [4]. Single-pass welds up to 28 mm wall thickness were conducted with an electromagnetic weld pool support system with a laser power of just 19 kW [5]. HLAW with cut-wire, which was filled in an air gap between the workpieces before welding, single-pass welds up to 25 mm with a ceramic or flux backing, and 50 mm in a double-sided welding technique were all realized successfully [6]. In [7], the HLAW process was demonstrated for one-side welding of steels with thicknesses of 28 mm to 32 mm in two to five layers, respectively. Alternatively, laser beam welding under a vacuum [8,9], laser submerged arc hybrid welding [10], or narrow-gap laser-arc hybrid welding [11] were successfully used for deep penetration welds.

It has been demonstrated that single-pass welds can be realized only at a sufficiently high welding speed, especially in a flat position, as soon as a full penetration is required. Otherwise, the increasing weld root width at reduced welding speeds leads to a reduction of the surface tension. In such a case, the surface tension cannot compensate for the hydrostatic pressure, which leads to the formation of inadmissible root defects such as drop-outs. The stability criterion is therefore dependent on the geometrical sizes of the weld seam, and is defined in accordance with [12] as follows:

$$h * w < 2 l_{cap}^2, \quad (1)$$

where h is the plate thickness, w is the root width, $l_{cap} = [\gamma/(\rho g_0)]^{1/2}$ is the capillary length, γ is the surface tension coefficient, ρ is the density of the melt, and g_0 is the gravitational acceleration. The geometrical sizes can be found in Figure 1a. The stability threshold for liquid steel with a density of $6.9 \times 10^3 \text{ kg m}^{-3}$ and a surface tension of 1.8 N m^{-1} is shown in Figure 1b.

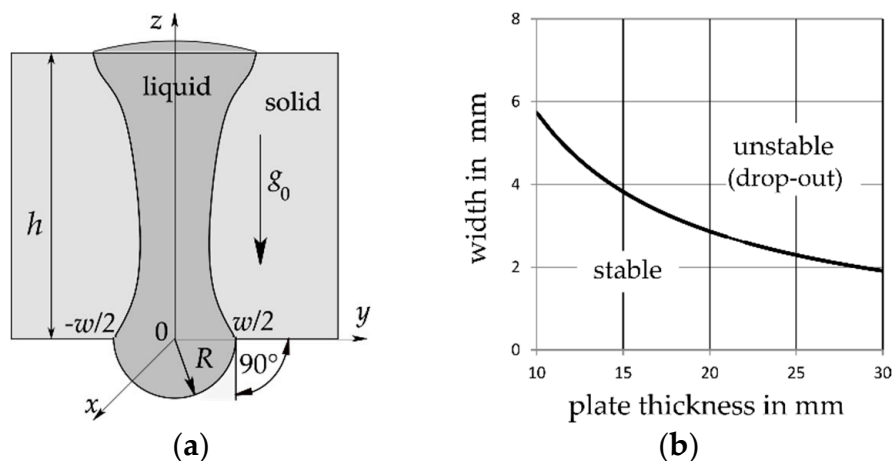


Figure 1. (a) Geometrical sizes of the weld pool, which influence the formation of droplets; (b) stability threshold for liquid steel, see Equation (1).

Another typical problem with deep penetration high-power HLAW is an insufficient and inhomogeneous distribution of the elements of the filler wire in the whole seam depth, which may lead to a deterioration of the mechanical properties, especially in the root part. The HLAW is characterized as a welding process with a reduced cooling time of only a few seconds. The additional energy of the arc welding process is not transported to the root part. So, a homogeneous filler wire mixing into the whole seam depth plays an important role in meeting the requirements of the mechanical

properties, especially for the welding of high-strength steels. In [13] it was shown that the filler wire had a homogeneous dilution of up to 3.7 mm, and 4.9 mm in a pulsed or modified spray using the arc operation mode of the gas metal arc welding process (GMAW). In a depth of approximately 13 mm, no content of the filler wire elements could be measured. Several studies were conducted to improve the filler wire mixing. The impact of the focal position of the laser beam on the characteristics of the melt flow and the weld pool geometry was demonstrated in [14]. With an air gap of 0.4 mm, the contents of the filler wire could also be observed in the root part. Nevertheless, the filler metal proportion in the weld was only 8% [15]. In [16], it was found that a trailing gas metal arc torch configuration helped in the mixing of the melt in the welding of 10 mm thick plates. The same approach was demonstrated in [17]. Moreover, a shielding gas containing more than 2% O₂ led to a homogeneous distribution of alloying elements in [17]. One of the main reasons for the inequitable distribution is caused by the Marangoni effect, which mainly influences the flow behavior near the surfaces. The peak values in the velocity magnitude are located on the free surfaces. This effect was shown numerically for LBW in [18,19]. Figure 2 shows the Ni concentration of a HLAW of a 10 mm thick steel plate. An unequal distribution can be clearly seen.

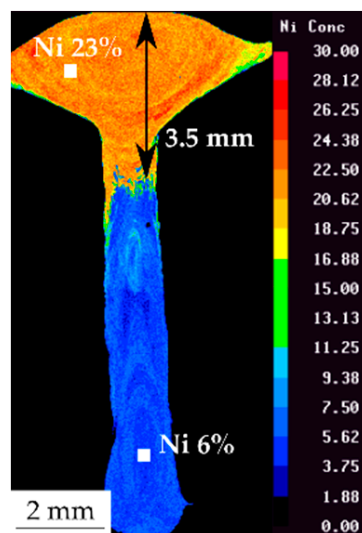


Figure 2. Nickel concentration of a hybrid laser-arc welding (HLAW) on a 10-mm-thick steel plate [20].

The electromagnetic stirring technique was used for the LBW of a 3-mm-thick aluminum plate, with an improvement of the element distribution [21–23]. The magnet was operated with a low-frequency in the range of 10–20 Hz. The objective of this research was to improve the element distribution and to prevent sagging with the use of oscillating magnetic fields for single-pass welds of thick plates.

2. Electromagnetic Weld Pool Influence

The electromagnetic weld pool support was demonstrated successfully for single-pass LBW [12] and for HLAW [24]. Figure 3 shows the AC electromagnetic weld pool support system used for the LBW or HLAW of thick metal parts. The AC magnet is located near the root side of the workpiece. The magnetic field B is directed perpendicular to the direction of welding. In this case, the induced current density j in the melt is directed along the welding direction, and the narrow gap between the welded parts does not affect the current density in the liquid metal. To estimate the current density in the melt, one can use the classical theory of the skin effect, see [25]. The resulting time-averaged

Lorentz force $F_L = j \times B$ is directed vertically and can provide support to the weld pool. The $F_L(z)$ decreases exponentially with increasing distance to the root surface of the sample, see Equation (2):

$$F_L(z) = \frac{B_0^2}{2\mu_0\delta} \exp\left(-\frac{2z}{\delta}\right), \quad (2)$$

where B_0 is the amplitude of the externally applied magnetic field, μ_0 is the magnetic field constant, and $\delta = (\pi \mu_0 \sigma f)^{-1/2}$ is the skin depth, where f is the AC frequency, σ is the electrical conductivity, and $\mu_0 = 1.257 \cdot 10^{-6} \text{ H m}^{-1}$ is the permeability of free space. The Lorentz force can be also expressed as a gradient of the electromagnetic pressure $F_L(z) = -\nabla p_{EM}(z)$. p_{EM} can be calculated as follows:

$$p_{EM}(z) = -\frac{B_0^2}{4\mu_0} \exp\left(-\frac{2z}{\delta}\right). \quad (3)$$

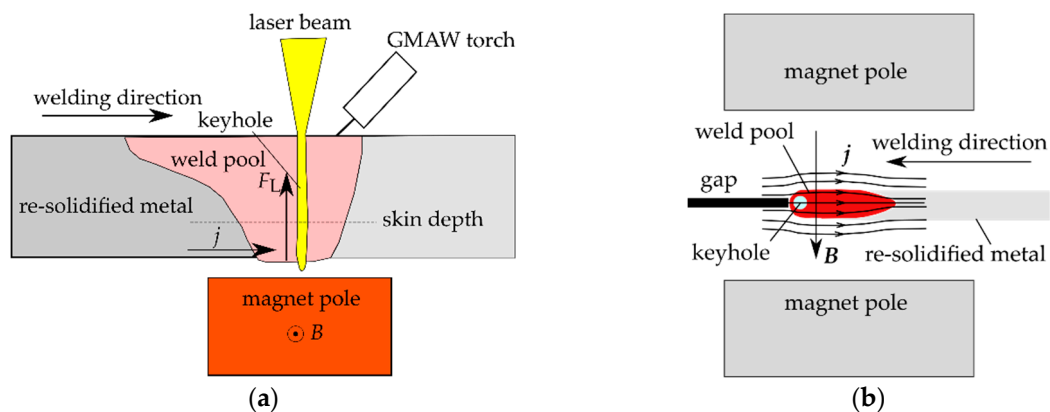


Figure 3. (a) Scheme of electromagnetic weld pool support system; (b) root side view of electromagnetic weld pool support system (the gap does not affect the current density). GMAW: gas metal arc welding.

For the conservative case, the magnetic field is perpendicular to the welding direction to generate a Lorentz force, whose potential component is counteracting the hydrostatic pressure as electromagnetic pressure. A rotational component of the Lorentz force is not given. The scheme of the electromagnetic weld pool support is shown in Figure 3a. The gap between the workpieces does not affect the current density in the weld pool, which is oriented in the welding direction (Figure 3b). This technology has been successfully used in the single-pass HLAW of steel plates with a thickness of up to 28 mm, with just 19 kW laser power [5]. When using hybrid laser-arc welding technology, it was necessary to choose a sufficiently high frequency of oscillation of the magnetic field so that the depth of penetration of the magnetic field into the metal would be significantly lower than the thickness of the sample board to be welded. A small part of the exponentially decaying magnetic field on the upper surface of the sample could affect the operation of the arc. This optimization was performed in [24], where it was shown that the amplitude of oscillation of the arc along the welding direction on the order of 1 mm did not have a significant effect on the weld shape geometry.

In the case of a turning of the magnetic field, a non-conservative component (vortical) of the Lorentz forces is formed in the weld pool due to the inhomogeneous course of the current and the concentration of the electric current in the weld pool. However, the electrical resistance in the joint gap is higher. The induced currents flow around the joint gap, which leads to the intensification of the flow lines at the boundary of the melt front (Figure 4a). The resulting Lorentz force has a rotational component which generates a vortical flow of the melt and causes a stirring effect of the melt and filler wire. In the case of turning the magnetic fields 90° to the welding direction, the compensation of the root reinforcement is not ensured. An optimal balance of electromagnetic weld pool support and electromagnetic stirring is found at a turn angle of 30° , see Figure 4b.

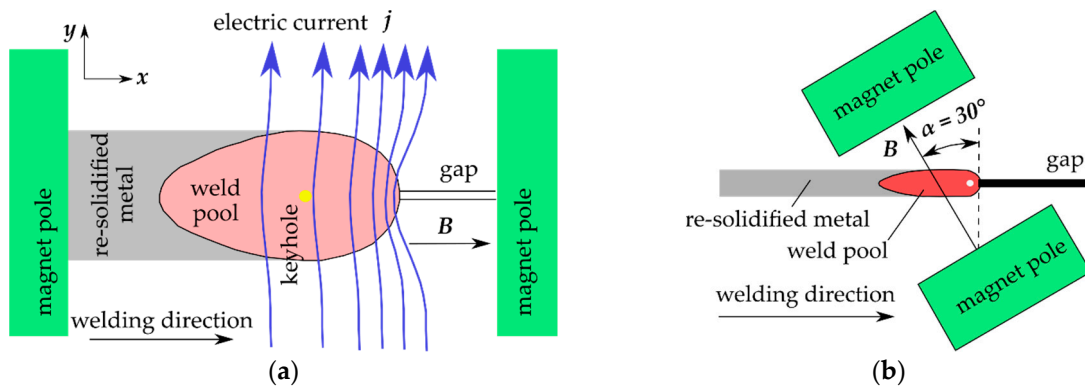


Figure 4. (a) Magnetic field parallel to the welding direction and influence of the electric current by the gap, non-conservative component of the Lorentz force; (b) optimal balance of conservative and non-conservative components of the Lorentz force at a turning through 30° .

3. Experimental Setup

The welding tests were executed in a flat position (1G) and in full penetration mode using a high-power fiber laser IPG YLR-20000 (IPG, Burbach, Germany) as a laser beam source, with a maximum output power of 20 kW, an emission wave length of 1070 nm, and a beam parameter product of $11 \text{ mm} \times \text{mrad}$. The laser radiation was transmitted through an optical fiber with a diameter of $200 \mu\text{m}$. A BIMO HP laser processing head from HIGHYAG (Kleinmachnow, Germany) with a focal length of 350 mm providing a spot focus diameter of 0.56 mm was also used. All tests were carried out with an arc leading orientation. The GMAW torch was tilted by 25° to the laser axis, which was positioned vertically in relation to the surface of the weld specimen. The laser beam was under-focused at 11 mm below the top surface of the weld specimen. The horizontal distance between the wire tip extension and the laser beam was 4 mm. Figure 5a shows the experimental setup.

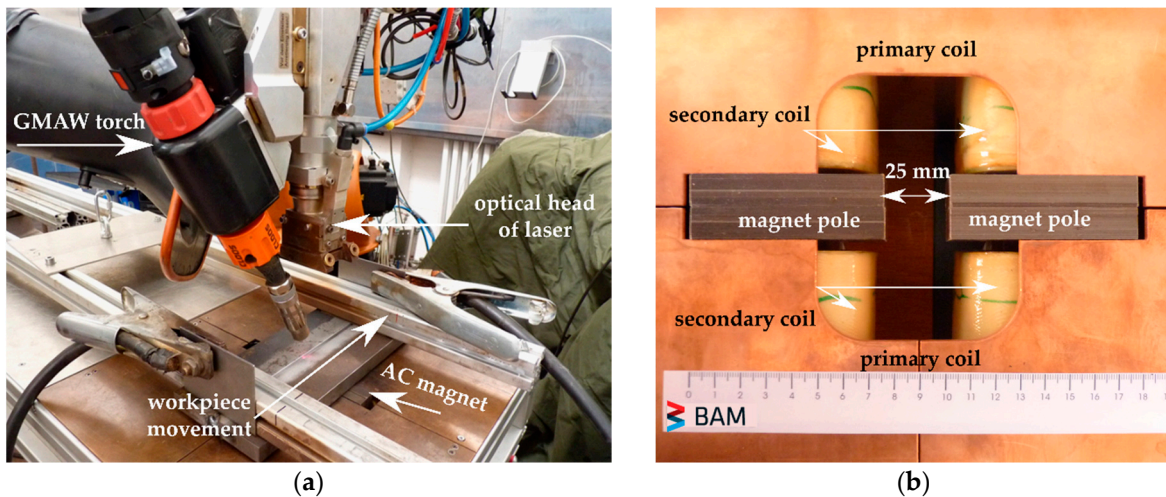


Figure 5. (a) Experimental setup; (b) AC magnet used for the experiments.

As a power source for the arc, a welding machine Qineo Pulse 600 (Cloos, Haiger, Germany) with a maximum current of 600 A was applied. An AC magnet providing a maximum output power of 6 kW was utilized at an oscillating frequency of 1.2 kHz. The electromagnet was positioned 2 mm below the workpiece. The distance between the two magnet poles was fixed to 25 mm. Figure 5b shows the AC magnet applied for the experiments.

The base material used for the experiments was a structural steel of grade S355J2 with a plate thickness of 20 mm. The joint was prepared as a single-Y joint with a root face of 14 mm and an opening angle of 45° . A nickel-based filler wire E Ni 6625 (NiCr22Mo9Nb), according to EN ISO 14172,

with a diameter of 1.2 mm was applied. This filler wire was deliberately chosen in order to produce a high-alloyed weld metal composition differing from the base metal. The welds were performed under gas shielding. The gas mixture consisted of 82% Ar and 18% CO₂ with a flow rate of 20 L min⁻¹. The chemical compositions of the base material and the filler wire are shown in Table 1.

Table 1. Chemical composition of materials used, shown in wt%.

Material/Element	C	Si	Mn	P	S	Cr	Ni	Mo	Cu	Nb	Fe
S355J2 ¹	0.08	0.29	1.3	0.019	0.004	-	-	-	0.008	-	bal.
E Ni 6625 ² (NiCr22Mo9Nb)	<0.04	<0.7	<1	-	-	21.5	bal.	9	-	3.3	<2

¹ measured by spectrum analyses at the BAM; ² according to the manufacturer specifications.

4. Results and Discussion

The metallographic evaluation of the cross sections shows that the electromagnetic pressure was capable of compensating for the hydrostatic pressure, as well as for the fully penetrated HLAW of 20-mm-thick S355J2 plates. The reference weld seam seen in Figure 6a shows that the hydrostatic pressure exceeded the surface tension and caused a drop-out of the molten metal. This seam is inadmissible according to the standard EN ISO 12932. With the use of an oscillating magnetic field, the weld shape formation corresponded to a typical wine-cup shape, and the sagging could be avoided as already shown in [5,24] (see Figure 6b). The AC magnet was operated at an oscillating frequency of 1.2 kHz and a magnet power of 1.8 kW. It was necessary to choose a sufficiently high frequency of oscillation for the magnetic field in order to protect the electric arc on the top surface. The groove was filled completely. The root excess weld metal was only 0.65 mm. The width on the root was 4.6 mm. According to the stability criterion (see Equation (1) and Figure 1b in accordance with [12]), an inadmissible sagging was to be expected without the use of any weld pool support. Using the electromagnetic weld pool support, the seam met the criteria for the highest evaluation, group B, according to EN ISO 12932. In this case, the direction of the magnetic field was perpendicular to the welding direction. This was in order to investigate only the effect of the weld pool support without the rotational component of the Lorentz force and a vortical flow. Figure 6c shows a cross section of a HLAW on a 20-mm-thick plate, where the magnetic field was turned through 30° relative to the welding direction. An additional component of the Lorentz force was generated. It can be seen that this seam also met the criteria for the highest evaluation group according to the EN ISO 12932 standards. The root was ideally compensated. The AC magnet power had to be adjusted to 2.3 kW, as part of the power was dissipated to generate a non-conservative (vortical) component of the Lorentz force. All seams were welded in full penetration mode with an arc leading orientation at a welding speed of 0.5 m min⁻¹, using 12.2 kW laser power and a wire feeding rate of 11 m min⁻¹.

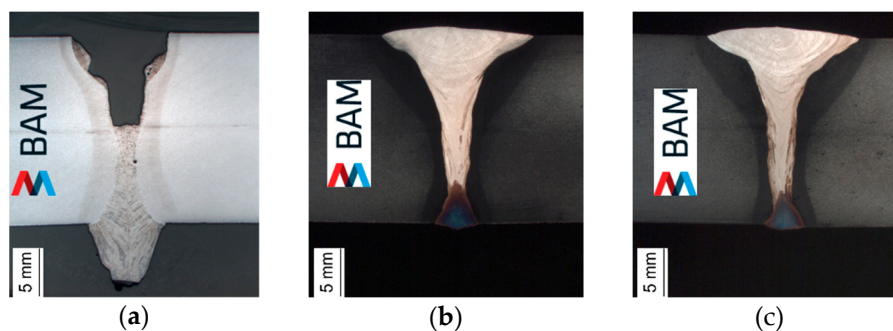


Figure 6. Cross sections of HLAW on 20-mm-thick plates of S355J2 using 12.2 kW laser power and wire feeding rate 11 m min⁻¹, at a welding speed of 0.5 m min⁻¹: (a) without electromagnetic weld pool support; (b) with electromagnetic support only (magnetic field perpendicular to the welding direction); (c) with electromagnetic support and stirring (magnetic field turned through 30°).

The analyses of the element distribution and quantity within the welded cross-section was identified using EDS. Chromium and nickel were the investigated elements. In the case of electromagnetic support only, the element distribution within the welded cross-section and over its entire thickness was inhomogeneous. In the upper part, a nickel content of 15.9 wt% was measured. In the middle and root parts, the nickel content was decreased to 12.3 wt% and 5.3 wt% respectively. To a maximum depth of 10 mm, the reduction of the element content was uncritical. Similar findings were obtained by Rethmeier et al. [20]. The nickel content in the root part amounted to one-third of the nickel content in the upper part. The same applies for the second tracing element chromium. This indicates that the filler wire was not mixed into the whole material thickness.

The next series of welding tests was performed with the AC magnet turned by $\alpha = 30^\circ$. The EDS data demonstrate an improvement in the homogeneity in the filler material distribution. In the upper part nickel and chromium contents of 8.2 wt% and 2.8 wt% were measured, respectively. In the middle part, the nickel content and the chromium content were 7.2 wt% and 2.6 wt%, respectively. A residual nickel content of 7.6 wt% was determined in the root part. A chromium content of 2.6 wt% was also detected in the root part. In general, the relative variation of the content of both tracing elements over the entire thickness of the weld seam did not exceed 4%.

Figure 7 shows the different zones for the determination of the nickel and chromium content by the EDS analysis.

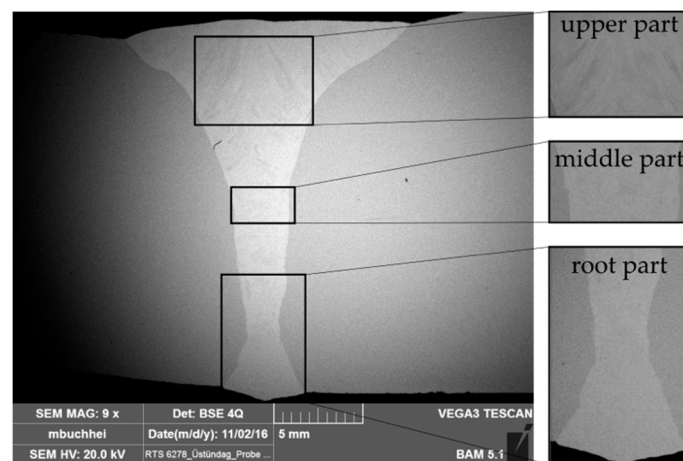


Figure 7. Schematic drawing of the different zones for results of the EDS analysis.

Figures 8 and 9 show the element distribution of the two tracing elements chromium and nickel within the weld seam in two different zones (upper part and root part) for the conservative (electromagnetic (EM) weld pool support only) and non-conservative case (EM support and stirring) of the magnetic weld pool influence, respectively.

It is clear that the vortical flow generated by a non-conservative component of the Lorentz force led to a radical improvement of the filler wire dilution over the entire weld seam thickness. This finding can lead to an improvement of the mechanical properties of single-pass hybrid laser-arc welds of thick structures. Since the HLAW process is still used for the welding of plates with a thickness up to 15 mm for industrial applications, this phenomenon was not deeply investigated. A homogeneous filler material distribution becomes important, especially at the single-layer HLAW of thicker materials and during the welding of modern thermomechanical rolled high-strength steels or cryogenic steels. One of the main reasons for the inhomogeneous mixing of the filler wire is explained by Marangoni convection, which mainly influences the flow behavior near the surfaces, which was discussed in detail in [18,19]. For that reason, a mixture of the filler wire did not take place. The filler wire was inserted into the process on the top side. Due to the rotational component of the Lorentz force, a vortical flow was generated, which led to an improvement in this situation.

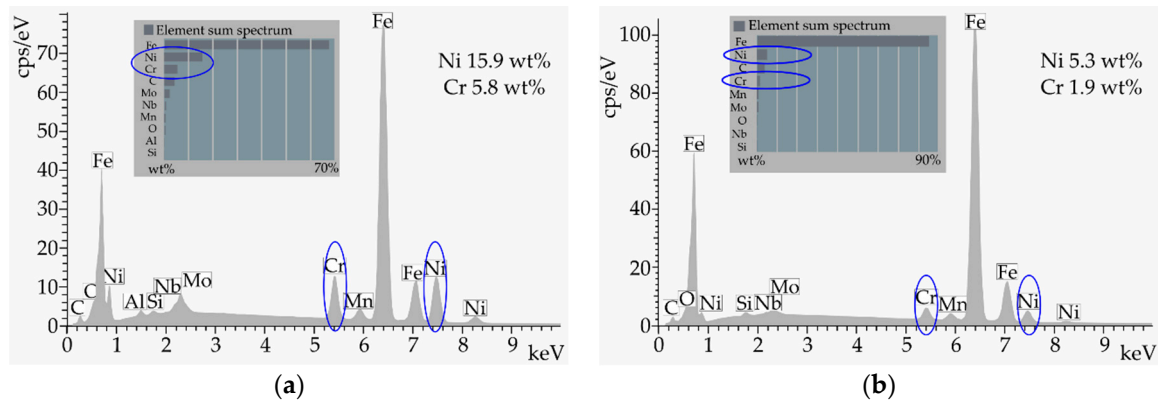


Figure 8. Results of the EDS analysis for the distribution of two tracing elements nickel and chromium of a HLAW 20 mm thick S355J2 with electromagnetic weld pool support (magnetic field perpendicular to the welding direction): (a) upper part; (b) root part.

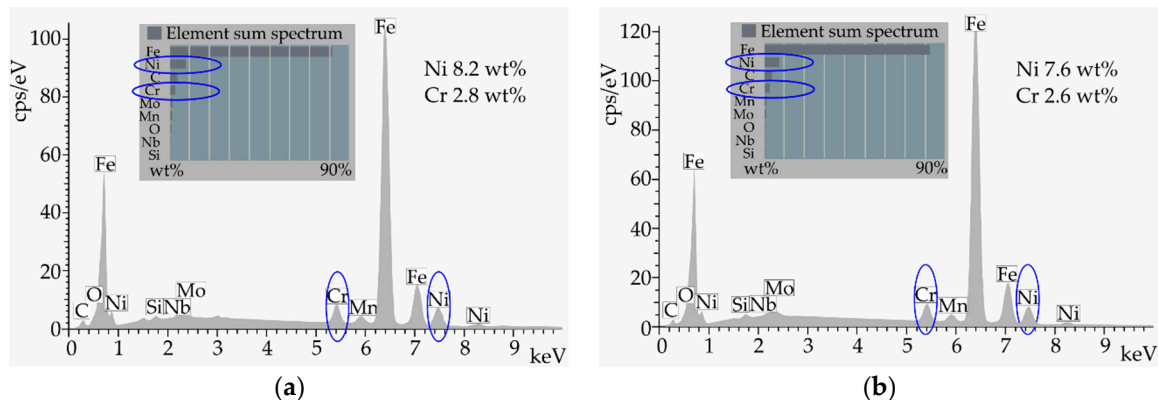


Figure 9. Results of the EDS analysis for the distribution of the two tracing elements nickel and chromium of a HLAW 20 mm thick S355J2 with electromagnetic weld pool support and stirring (magnetic field turned through 30° to the welding direction): (a) upper part; (b) root part.

5. Conclusions

Full penetration HLAW tests for 20-mm-thick S355J2 steel plates were performed for different designs of the orientation of external oscillating magnetic fields. A magnetic field perpendicular to the welding direction was successfully used for weld pool support. An AC power of 1.8 kW at an oscillating frequency of 1.2 kHz was necessary to prevent sagging and gravity drop-outs for single-pass HLAW. The seams could be classified in the highest evaluation group B according to EN ISO 12932. By turning the magnetic field 30°, a non-conservative (rotational) component of the Lorentz force was generated, which was used for the electromagnetic stirring of the filler wire. The EDS analyses confirmed that the rotational component of the Lorentz force led to a radical improvement in the homogeneity of the filler material distribution over the entire weld seam depth. The adaptation of the electromagnetic weld pool support and stirring can dramatically increase the application potential of the hybrid laser-arc welding process.

Author Contributions: The experiments were conducted by Ö.Ü. Discussion and conclusions were written with the contribution of all authors.

Funding: This research received no external funding.

Acknowledgments: The authors would like to thank Michaela Buchheim (Division 5.1 Materialography, Fractography and Ageing of Engineered Materials at the Bundesanstalt für Materialforschung und -prüfung) for the performing of the EDS analysis.

Conflicts of Interest: The authors declare no conflict of interest.

References

1. Eboo, M.; Steen, W.M.; Clarck, J. Arc augmented laser processing of materials. In Proceedings of the International Conference of Advances in Welding Processes, Harrogate, UK, 9–11 May 1978.
2. Roland, F.; Manzon, L.; Kujala, P.; Brede, M.; Weitzenböck, J. Advanced joining techniques in European shipbuilding. *J. Ship Prod.* **2004**, *20*, 200–210.
3. Gumenyuk, A.; Rethmeier, M. Developments in hybrid laser-arc welding technology. In *Handbook of Laser Welding Technologies*; Katayama, S., Ed.; Woodhead Publishing Ltd.: Cambridge, UK, 2013; pp. 505–521.
4. Bachmann, M.; Gumenyuk, A.; Rethmeier, M. Welding with high-power lasers: trends and developments. *Phys. Procedia* **2016**, *83*, 15–25. [[CrossRef](#)]
5. Üstündag, Ö.; Avilov, V.; Gumenyuk, A.; Rethmeier, M. Full penetration hybrid laser arc welding of up to 28 mm thick S355 plates using electromagnetic weld pool support. *J. Phys. Conf. Ser.* **2018**, *1109*, 12–15. [[CrossRef](#)]
6. Wahba, M.; Mizutani, M.; Katayama, S. Single pass hybrid laser-arc welding of 25 mm thick square groove butt joints. *Mater. Des.* **2016**, *97*, 1–6. [[CrossRef](#)]
7. Rethmeier, M.; Gook, S.; Lammers, M.; Gumenyuk, A. Laser-hybrid welding of thick plates up to 32 mm using a 20 kW fibre laser. *J. Jpn. Weld. Soc.* **2009**, *27*, 74–79. [[CrossRef](#)]
8. Katayama, S.; Yohei, A.; Mizutani, M.; Kawahito, Y. Development of deep penetration welding technology with high brightness laser under vacuum. *Phys. Procedia* **2011**, *12*, 75–80. [[CrossRef](#)]
9. Reisinger, U.; Olschok, S.; Longerich, S. Laser Beam Welding in Vacuum—A Process Variation in Comparison with Electron Beam Welding. In Proceedings of the 29th International Congress on Applications of Lasers & Electro-Optics ICALEO 2010, Anaheim, CA, USA, 26–30 September 2010; pp. 637–638.
10. Reisinger, U.; Olschok, S.; Jakobs, S. Laser submerged arc welding (LUPuS) with solid state lasers. *Phys. Procedia* **2016**, *56*, 653–662. [[CrossRef](#)]
11. Zhang, C.; Li, G.; Gao, M.; Zeng, X. Microstructure and mechanical properties of narrow gap laser-arc hybrid welded 40 mm thick mild steel. *Materials* **2017**, *10*, 106. [[CrossRef](#)]
12. Avilov, V.; Gumenyuk, A.; Lammers, M.; Rethmeier, M. PA position full penetration high power laser beam welding up to 30 mm thick AlMg3 plates using electromagnetic weld pool support. *Sci. Technol. Weld. Joining* **2012**, *17*, 128–133. [[CrossRef](#)]
13. Gook, S.; Gumenyuk, A.; Rethmeier, M. Hybrid laser arc welding of X80 and X120 steel grade. *Sci. Technol. Weld. Joining* **2014**, *19*, 15–24. [[CrossRef](#)]
14. Schaefer, M.; Kessler, S.; Fetzer, F.; Graf, T. Influence of the focal position on the melt flow during laser welding of steel. *J. Laser Appl.* **2017**, *29*, 012010. [[CrossRef](#)]
15. Karhu, M.; Kujanpaa, V.; Gumenyuk, A.; Lammers, M. Study of filler metal mixing and its implication on weld homogeneity of laser-hybrid and laser cold-wire welded thick austenitic stainless steel joints. In Proceedings of the International Congress on Applications of Lasers & Electro-Optics 2013, Miami, FL, USA, 6–10 October 2013; pp. 252–261.
16. Sohail, M.; Karhu, M.; Na, S.J.; Han, S.W.; Kujanpaa, V. Effect of leading and trailing torch configuration on mixing and fluid behavior of laser-gas metal arc hybrid welding. *J. Laser Appl.* **2017**, *29*, 042009.
17. Zhao, L.; Sugino, T.; Arakane, G.; Tsukamoto, S. Influence of welding parameters on distribution of wire feeding elements in CO₂ laser GMA hybrid welding. *Sci. Technol. Weld. Joining* **2009**, *14*, 457–467. [[CrossRef](#)]
18. Bachmann, M.; Avilov, V.; Gumenyuk, A.; Rethmeier, M. Experimental and numerical investigation of an electromagnetic weld pool support system for high power laser beam welding of austenitic stainless steel. *J. Mater. Process. Technol.* **2014**, *214*, 578–591. [[CrossRef](#)]
19. Bakir, N.; Artinov, A.; Gumenyuk, A.; Bachmann, M.; Rethmeier, M. Numerical simulation on the origin of solidification cracking in laser welded thick-walled structures. *Metals* **2018**, *8*, 406. [[CrossRef](#)]
20. Rethmeier, M.; Gook, S.; Gumenyuk, A. Einsatz des Laserstrahl-MSG-Hybridschweißverfahrens an längsnahtgeschweißten Großrohren der Güte API-X80/-X100 zur Steigerung der Zähigkeit und Erhöhung der Wirtschaftlichkeit. In *FOSTA Bericht P822*; Forschungsvereinigung Stahlanwendung e.V.: Düsseldorf, Germany, 2012.
21. Gatzen, M.; Tang, Z.; Vollertsen, F. Effect of electromagnetic stirring on the element distribution in laser beam welding of aluminium with filler wire. *Phys. Procedia* **2011**, *12*, 56–65. [[CrossRef](#)]

22. Tang, Z.; Gatzen, M. Influence on the dilution by laser welding of aluminum with magnetic stirring. *Phys. Procedia* **2010**, *5*, 125–137. [[CrossRef](#)]
23. Vollertsen, F.; Thomy, C. Magnetic stirring during laser welding of aluminum. *J. Laser Appl.* **2006**, *18*, 28–34. [[CrossRef](#)]
24. Üstündağ, Ö.; Fritzsche, A.; Avilov, V.; Gumenyuk, A.; Rethmeier, M. Hybrid laser-arc welding of thick-walled ferromagnetic steels with electromagnetic weld pool support. *Weld. World* **2018**, *62*, 767–774. [[CrossRef](#)]
25. Landau, L.D.; Lifshitz, E.M. Course of Theoretical Physics. In *Electrodynamics of Continuous Media*; Butterworth-Heinemann: Oxford, UK, 1984.



© 2019 by the authors. Licensee MDPI, Basel, Switzerland. This article is an open access article distributed under the terms and conditions of the Creative Commons Attribution (CC BY) license (<http://creativecommons.org/licenses/by/4.0/>).